

# DMD WITH LOW RANK FEATURE COMPRESSION FOR VIDEO BACKGROUND EXTRACTION \*

HAOZE HE

**1. Introduction.** DMD, a mathematical method that was developed to understand the evolution of a dynamical system without prior knowledge of their governing equations, proves to be well-suited for extracting insights from real-world data captured as snapshots over time. Video data falls into this scheme, and therefore DMD is a suitable method to understand video data. Additionally, another property of DMD, which we will delve into later, is the higher the dimension of the snapshot/observation/measurement is, the better DMD can understand or reconstruct the underlying dynamics. Video data typically falls into this category, with each frame representing an image residing in a high-dimensional Euclidean space. The specific focus of this report is on background extraction in video learning tasks.

## 2. DMD and video background extraction.

**2.1. DMD.** Consider a discrete dynamical system

$$z_i = T(z_{i-1})$$

17 where the states  $z_i, i = 0, 1, \dots$  lie in a state space  $\mathcal{X}$ . Consider observables (e.g.,  
 18 measurements)  $f \in \mathcal{F} : \mathcal{X} \rightarrow \mathbb{C}$  and we define the Koopman operator, which is a key  
 19 concept of DMD, as follows:

$$\mathcal{K}f(z_i) = f(T(z)) = f(z_{i+1}).$$

21 By its definition,  $\mathcal{K}$  is linear, and if the space of observables  $\mathcal{F}$  is “nice” enough,  
 22 (e.g.,  $\mathcal{F} \subseteq L^2(X, \mu)$ ),  $\mathcal{K}$  has a discrete spectral decomposition, and DMD is a way to  
 23 approach this spectral decomposition given only snapshot data of the dynamics.

Let  $S = [s_1 \cdots s_n] \in \mathbb{C}^{d \times n}$  be the snapshots, that is,  $s_i = [f_1(z_i) \cdots f_d(z_i)]$ ; they are the measurements of the states  $z_1, \dots, z_n$ . Let  $X = S(1 : n - 1)$ ,  $Y = S(2 : n)$ , our task is to find a best fit matrix  $A$  such that  $\|X^T A - Y^T\|_F$  is as small as possible. Mathematically, one of the optimal  $A$  can be computed by  $A = (YX^\dagger)^T$  where  $\dagger$  denotes the pseudo-inverse. However, computing the pseudo-inverse of a rank-deficient matrix is unstable. To avoid the ill-conditioness, we apply the Schmid DMD. Let  $U_k \Sigma_k V_k^H$  be the truncated rank- $k$  SVD of  $X$ , the Schmid DMD computes an approximation of  $A^T$  in  $\text{span}\{U_k\}$  as

$$A^T = U_k U_k^H Y (U_k \Sigma_k V_k^H)^\dagger U_k = U_k^H Y V_k \Sigma_k^{-1}.$$

<sup>33</sup> We also provide our own DMD implementation with normalization.

34 The above computational approach in finite dimension has its counter part in functional space. It is equivalent to first restrict  $\mathcal{K}$  to the subspace spanned by  $f_1, \dots, f_d$   
 35 where we assume

$$s_i = [f_1(t_i) \cdots f_d(t_i)]^T,$$

38 with  $f_1, \dots, f_d$  are not fully known but only known their evaluations at  $t_1, \dots, t_n$  (we  
 39 can think of  $t_i$  as time). After the restriction, the above DMD approach corresponds

\*Joint work with Nian Shao.

40 to the following least square problem

41

$$\int |fA - \mathcal{K}f|^2 d\delta_N$$

42 where  $\delta_N$  is the discrete measure,  $f = [f_1 \cdots f_d]$  is a quasi-matrix in the sense of [5].  
 43 From this discussion, we can expect that our computed  $A$ 's eigenvalues approximate  
 44 the true eigenvalues of  $\mathcal{K}$  better and better with more snapshots (i.e., more time steps  
 45 so that the discrete measure approximates the underlying measure of the sample  
 46 space) and more observables (i.e., larger subspaces so that the restricted map approx-  
 47 imates the original map). Then the eigenvalue of  $A$  is the approximated eigenvalues  
 48 of  $\mathcal{K}$  with Rayleigh-ritz procedure to restrict to  $\text{span}\{f_1, \dots, f_d\}$ .

49 Let  $A = Q\Lambda Q^{-1}$  be the corresponding eigenvalue decomposition of  $A$ . From the  
 50 minimization process, we know that

51

$$\mathcal{K}f \approx fA,$$

52 thus,

53

$$\mathcal{K}fQ \approx fQ\Lambda,$$

54 and we know that  $\phi = [\phi_1 \cdots \phi_d] = fQ$  are the approximated eigenfunctions of  $\mathcal{K}$ . But  
 55 they are only known to us at the given snapshots, i.e., we only know  $\phi(t_1), \dots, \phi(t_n)$ .

56 Then we can express the partially known observables  $f$  in terms of  $\phi$ ,

57

$$f^T = Q^{-T}(fQ)^T = Q^{-T}\phi^T = \sum z_i\phi_i$$

58 where  $z_i$  is the  $i$ th columns of  $Q^{-T}$ . Then it follows straightforwardly to obtain the  
 59 so-called koopman mode decomposition

60

$$\mathcal{K}^k f^T(s_1) \approx \sum z_i\phi_i(s_1)\lambda_i^k.$$

61 The vector  $z_i\phi_i(s_1)$  has key information of our dynamical system, especially for the  
 62 task of video background extraction, which will be discussed in the following subsec-  
 63 tion.

64 **2.2. Video background extraction.** Consider the vector  $z_i$ , each entry of  $z_i$ ,  
 65  $z_i(j)$ , is the component that how much of  $f_j$  belongs to the eigenfunction  $\phi_i$ , if we  
 66 collect all of these component into one vector  $z_i \in \mathbb{C}^d$ , it extracts the component that  
 67 how our snapshot  $f = [f_1 \cdots f_d]$  belongs to the  $i$ th eigenfunction  $\phi_i$ . Note that this  
 68 vector  $z_i$  will envolve with respect to time in the same way as the eigenfunction  $\phi_i$   
 69 envolve with respect to the koopman operator  $\mathcal{K}$  by the formula

70

$$\mathcal{K}^k f^T(s_1) \approx \sum z_i\phi_i(s_1)\lambda_i^k.$$

71 That is, we decompose the whole dynamical system in terms of the individual envo-  
 72 lution of the components corresponding to each eigenfuction  $\phi_i$ .

73 Consider our data now as video and each snapshot is an image, the  $z_i$  vector is  
 74 also an image. It captures how much each frame can be decomposed into different  
 75 eigenfuntcion  $\phi_i$ . But we can have physical interpretation for  $z_i$  in terms of video.  
 76 Imagine one extreme case that  $\phi_1$  has eigenvalue 1, then the component that corre-  
 77 sponding to  $\phi_1$ ,  $z_1$ , will not change with respect to time, i.e.,  $z_i$  capture the unmoved  
 78 component in the video, which by definition, is the background. For the component

79 vector  $z_i$  that corresponds to an eigenvalue of  $\mathcal{K}$  with a large negative real part, it will  
 80 decay rapidly and therefore corresponding to the object that disappear quickly in the  
 81 video. For example, when a car go pass by a section of the highway, we can expect  
 82 that the components that corresponding to the car, if we express them in koopman  
 83 modes, shall correspond to eigenvalues with large negative real parts. On the other  
 84 hand, the components that corresponding to the road should close to 1. These key  
 85 observation provide us with a criteria to select koopman modes as background or  
 86 foreground; we can look at the quantity  $|\log(\lambda_i)|$ , if this quantity is small, meaning  
 87 that the corresponding koopman mode has approximated eigenvalue close to 1, which  
 88 is more likely to correspond to the background.

89 **3. Our approach.**

90 **3.1. Low rank image patches.** For video data, one major challenge is that  
 91 each frame is a image with a very high dimension, e.g.,  $1920 \times 1080$ . To efficiently  
 92 perform DMD even in real time, we should compress our video data. In [1–3], random-  
 93 ized SVD (RSVD) are proposed to replace the original SVD in the DMD computation  
 94 to reduce the complexity. However, they all consider the standard vectorization of  
 95 images, which might destroy the connection between nearby pixels within one frame  
 96 . This problem is addressed in [4] by dictionary learning, where images are divided  
 97 into small patches, and for each small patch, a dictionary is learnt from the whole  
 98 video, and in each frame, we only extract the coefficients of the corresponding com-  
 99 ponents in the dictionary, this reduces the dimension and keep the local coherence of  
 100 the pixels. However, in [4], the process of the dictionary learning is solved by very  
 101 expensive iterative optimization method, which is much more expensive than the full  
 102 DMD directly to frames.

103 In this report, we propose Low Rank Image Patch. It is based on the observation  
 104 that if we vectorize each patch, stack each vectorized patch at different frames in the  
 105 video into a short and fat matrix, this matrix is expected to be low rank, as for each  
 106 patch, it is very unlikely to change dramatically with respect to time, (e.g., consider  
 107 a car passing by a section of a road), and therefore we can use only a few basis vector  
 108 to approach the range. This procedure is summarized as follows

---

**Algorithm 3.1** Low Rank Patch Extraction (LRPE)

---

**Input:** A video  $V \in \mathbb{R}^{m \times n \times T}$ , # of patches  $N$ , rank  $r$ ,  
**Output:**  $r$  basis vectors of each patch, in total  $r \times N$  vectors.

1: **for**  $i = 1$  to  $N$   
 2:   extract patch  $i$ ,  $p_i(k)$  for  $V(:, :, k)$ ,  $k = 1, \dots, T$ ,  
 3:    $A = [p_i(1), \dots, p_i(T)]$   
 4:   compute top  $r$  left singular vectors of  $A$  and keep them for output  
 5: **end for**

---

109 After finding the basis vectors, we only need to run DMD on the coefficient of  
 110 each patch with respect to the corresponding basis vectors. That is, we perform usual  
 111 DMD on the vectorization of the coefficients of each patch.

**Algorithm 3.2** LRPE DMD

**Input:** A video  $V \in \mathbb{R}^{m \times n \times T}$ , basis vectors of  $N$  patches  $Q_1, \dots, Q_N$

```

1: for  $i = 1$  to  $N$ 
2:   extract patch  $i$ ,  $p_i(k)$  for  $V(:, :, k)$ ,  $k = 1, \dots, T$ ,  $C_i(k) = Q_i^T p_i(k)$ 
3: end for
4: Run DMD on  $[[C_1(1) \dots C_N(1)]^T \dots [C_1(T) \dots C_N(T)]^T]$ .

```

**3.2. Iterative refinement.** It is possible to refine the result by iteratively running DMD on the residual after extracting the background, to capture more part of moving background in the resulting foreground, as suggested in [1].

However, we find out that if we do not do truncation in solving the least square problem in DMD, we should expect identical result among different refinement iteration. If we have

$$A = YX^\dagger$$

and obtain the first background as

$$B = [v_1 \ \cdots \ v_n].$$

Divide  $B$  into

$$B_1 = [v_1 \ \cdots \ v_{n-1}], \quad B_2 = [v_2 \ \cdots \ v_n] = AB_1$$

and subtract them from the original snapshots we get

$$X' = X - B_1, \quad Y' = Y - AB_1.$$

We will have

$$Y'X'^\dagger = A.$$

However, if we truncate the SVD when we solve the least square problem in DMD, which corresponds to throwing away information we do not trust, we can expect improvement from the.

**4. Numerical results.** All numerical experiments in this section are implemented in Matlab 2022b and executed with an AMD Ryzen 9 6900HX Processor (8 cores, 3.3–4.9 GHz) and 32 GB of RAM. We apply our novel DMD background extraction method to two real videos, one is of small size ( $90 \times 72$  resolution) and the other is of large size ( $852 \times 480$  resolution). We also compared our implementation with the original implementation of dictionary learning [6] on the small size video, while on the large-size video, the original algorithm is too slow to produce an output within a reasonable time.

For the small-size video, we use their video as [Figure 4.1](#). Compared with their algorithm (using their public codes), we can achieve a  $484 \times$  speed-up, i.e., from 141.7 seconds to 0.2927 seconds. The background and foreground reconstructed are given in [Figures 4.2](#) and [4.3](#). Compared with their results, our method can recover a better foreground, i.e., two people are walking around.

Now we would like to discuss possible reasons for the superiority of low-rank approximation (our method) than dictionary learning (their method). Dictionary learning and sparse approximation are effective methods in signal processing. However, compared with signal, the video is much more complex and noiseless. In our setting, for each batch, there is no need to use a very large size of dictionary. Moreover, in our problem, we do not predict the further video, which means we have all

149 data in hand. In such a situation, truncated SVD is the best low-rank approximation,  
 150 especially when the video admits a low-rank structure. Thus, it is not surprise that  
 151 low-rank approximation will outperform dictionary learning.

152 For the large-size video (Figure 4.4), their method does not work; it does not  
 153 produce the result within a reasonable time. We sucessfully extract the background  
 154 keyboard of this instrument, as shown in Figure 4.5. We only show one image because  
 155 this does not change with respect to frames in this example.

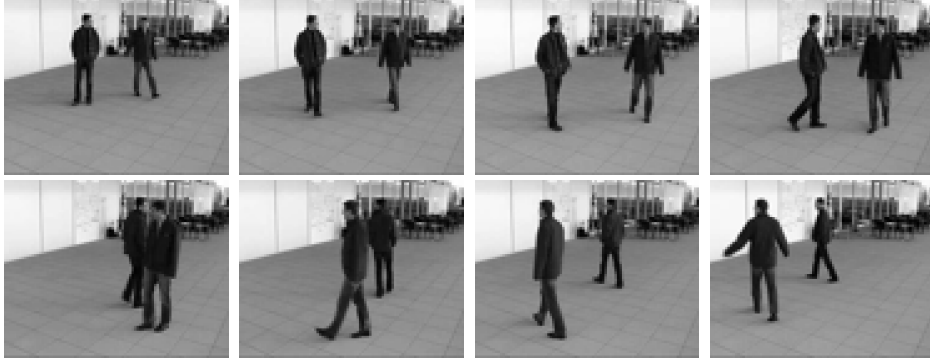


Fig. 4.1: Slice of small size video.



(a) Background



(b) Foreground

Fig. 4.2: Background and foreground recovered by our method.

156 **5. Conclusion.** In this report we present a novel DMD algorithm for video back-  
 157 ground extraction, and we demonstrate the intuition why low rank patch compression  
 158 can help improve both the accuracy and efficiency. We demonstrate our advantage  
 159 over the original improvement on real videos.

160 During the low rank patch compression phase, the current compression method  
 161 is standard SVD, but in this situation, the target rank is known to us, and therefore



(a) Background



(b) Foreground

Fig. 4.3: Background and foreground recovered by their method.

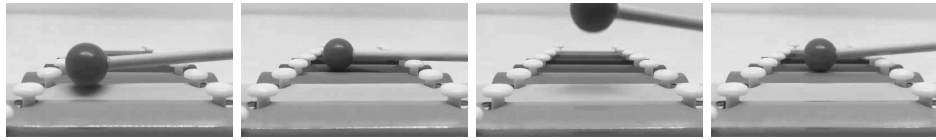
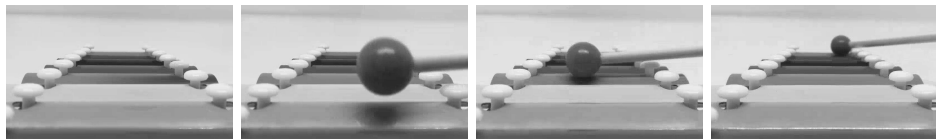


Fig. 4.4: Slice of small size video.

162 we expect Randomized SVD (RSVD) can significantly improve the efficiency without  
 163 too much loss of accuracy.

164 We also would like to extend our current algorithm into streaming setting to  
 165 capture the change of the background with respect to time, and this we need more  
 166 efficient implementation of compression (again, RSVD is suitable) and seek for SVD  
 167 or QR update to allow for streaming data.

168 We also expect that our work can be extended to video frames prediction.

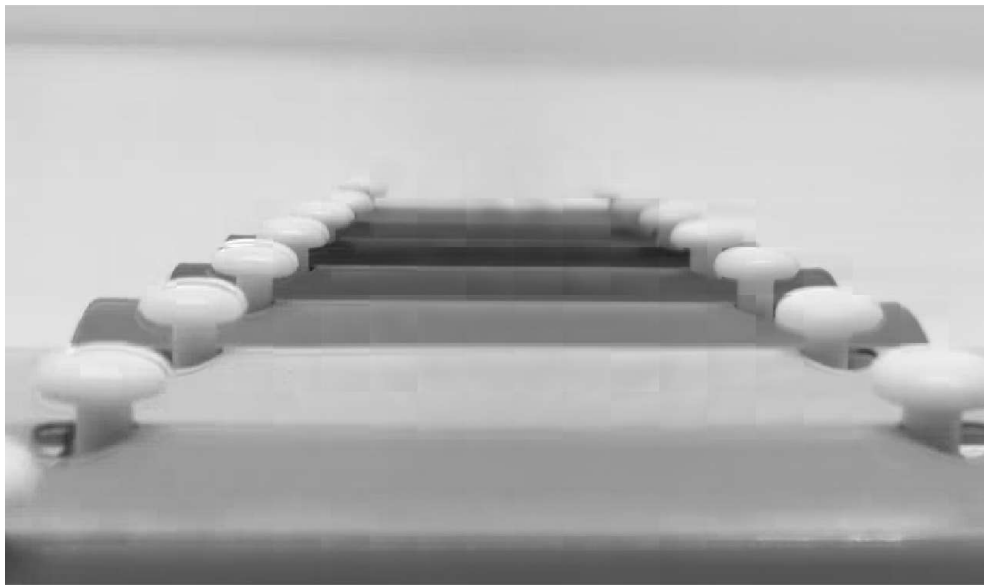


Fig. 4.5: Background of the large video

169

#### REFERENCES

170 [1] N. B. Erichson, S. L. Brunton, and J. N. Kutz. Compressed dynamic mode decomposition for  
171 background modeling. *Journal of Real-Time Image Processing*, 16(5):1479–1492, 2019.  
172 [2] N. B. Erichson and C. Donovan. Randomized low-rank dynamic mode decomposition for motion  
173 detection. *Computer Vision and Image Understanding*, 146:40–50, 2016.

174 [3] J. Grosek and J. N. Kutz. Dynamic mode decomposition for real-time background/foreground  
175 separation in video. *arXiv preprint arXiv:1404.7592*, 2014.

176 [4] I. U. Haq, K. Fujii, and Y. Kawahara. Dynamic mode decomposition via dictionary learning for  
177 foreground modeling in videos. *Computer Vision and Image Understanding*, 199:103022,  
178 2020.

179 [5] L. N. Trefethen. Householder triangularization of a quasimatrix. *IMA J. Numer. Anal.*,  
180 30(4):887–897, 2010.